

"This is the peer reviewed version of the following article: [International Journal for Numerical Methods in Engineering, 2018, 115 (6), pp. 695 - 713], which has been published in final form at [<https://onlinelibrary.wiley.com/doi/abs/10.1002/nme.5821>] This article may be used for non-commercial purposes in accordance with Wiley Terms and Conditions for Self-Archiving

# Robust topology optimization for cellular composites with hybrid uncertainties

Jing Zheng<sup>1,2</sup>, Zhen Luo<sup>1</sup>, Hao Li<sup>1</sup>, Chao Jiang<sup>2,\*</sup>

*\*Corresponding author*

Phone: +86731 88821445; Fax: +86 731 88822051; E-mail: [jiangc@hnu.edu.cn](mailto:jiangc@hnu.edu.cn) (Prof C. Jiang)

<sup>1</sup>*School of Mechanical and Mechatronic Engineering*

*University of Technology, Sydney, 15 Broadway, Ultimo, NSW 2007 Australia*

<sup>2</sup>*State Key Laboratory of Advanced Design and Manufacturing for Vehicle Body*

*School of Mechanical and Vehicle Engineering*

*Hunan University, Changsha, Hunan Province, 410082, China*

**Abstract:** This paper will develop a new robust topology optimization method for the concurrent design of cellular composites with an array of identical microstructures subject to random-interval hybrid uncertainties. A concurrent topology optimization framework is formulated to optimize both the composite macrostructure and the material microstructure. The robust objective function is defined based on interval mean and interval variance of the corresponding objective function. A new uncertain propagation approach, termed as a hybrid univariate dimension reduction (HUDR) method, is proposed to estimate the interval mean and variance. The sensitivity information of the robust objective function can be obtained after the uncertainty analysis. Several numerical examples are used to validate the effectiveness of the proposed robust topology optimization method.

**Key Words:** Topology optimization, hybrid uncertainties, multi-scale design, dimension-reduction method

## 1. Introduction

Structural engineers always endeavor to search for more efficient use of material so as to make structures as light as possible yet able to bear loads. Structural optimization has been developed as such a computational design tool that makes it possible to find optimized structures via numerical procedures. In particular, topology optimization has been experiencing great popularity in the last two decades due to the savings in material usage and performance gains in structures. Topology optimization actually provides a numerical iterative process that can automatically redistribute a given amount of materials within a reference design

domain under appropriate boundary conditions, so as to optimize the concerned structural performance. Since the work [1], a series of methods have been developed for topology optimization of structures, such as the solid isotropic material with penalization (SIMP) [2,3], evolutionary structural optimization (ESO) [4,5], and level set methods (LSM) [6,7,8,9]. More comprehensive reviews for topology optimization over the past decades can be referred to [10,11,12].

Most conventional topology optimization methods are focused on the use of full solid materials with certain properties, which limits the capacity of topology optimization for more advanced designs and applications in order to search for lightweight but high performance structures. Periodic cellular composites are modular materials that are assembled by incorporating heterogeneous elements with functions determined by their relatively smaller placements like microstructures or unit cells. Each cell consists of an optimized layout of material, allowing arbitrary topological changes of the microstructure. The assembled cellular composites introduce a new degree of freedom and the global multifunctional properties can be determined from the local configurations of heterogeneous cells. Such composite materials can improve efficiency by reducing weight while gaining high-performance for given strength and stiffness or etc. Hence, the importance of cellular composites has grown rapidly in engineering [13]. Cellular composites provide flexibility in implementing effective properties by only modifying microscopic cells rather than their constituents. However, it can be seen that the current designs for cellular composites are mostly focused on microstructures [14,15,16,17], and the property of the macro structure is seldom included in the framework of an integrated or concurrent design.

There have been some topology optimization methods for the concurrent design of the host macrostructure and its microstructures, namely the composite macrostructure and material microstructure that are optimized simultaneously. The concurrent topology optimization aims at designing the structures composed of cellular composites on the micro scale and the macro scale simultaneously according to the given boundary conditions. The layouts of materials can then be optimized to a large extent and the structure performance can be expected to be the best. The multiscale lightweight cellular composites provide new opportunities in many advanced engineering applications (e.g. bioengineering materials) [18,19], and may enhance the structural performances (e.g. thermal and thermo-elastic effects) [20,21]. Rodrigues et al. [22] developed a hierarchical computational procedure for optimizing the macrostructure material distribution as well as designing the point-wise material microstructures, in which allows unique microstructure in each macro finite element. However, microstructural variations from point to point in the macro scale may cost large calculation and result in manufacturing difficulties. In this case, periodic assumption is often made in order to meet the computational design and manufacturing requirements in practice. Based on this periodic assumption, the macroscopic composite structure is often assumed to have an array of identical microstructures that are periodically configured with the same shape and topology. Liu et al. [23] proposed a

so-called PAMP (Porous Anisotropic Material with Penalization) model to optimize the macroscopic and microscopic material distributions simultaneously. In [24], composite material involving two or three different material phases was designed by using the homogenization method to minimize the mean compliance of the macrostructure. There have been more works focused on integrated designs of various types of cellular composites, e.g. thermoelastic problems [25] and frequency response analysis problems [26], and functionally graded cellular composites [27]. However, in most of the above designs, uncertainties haven't been considered in the formulations of topology optimization problems.

In engineering, various uncertainties due to variations triggered by manufacturing tolerances, loadings, material properties, fabrication tolerances, and geometric dimensions unavoidably exist in practical design applications [28]. There have been two different types of uncertainties, namely the aleatory and epistemic uncertainties. The former uncertainty which is also named as objective or stochastic uncertainty describes the inherent variation of a physical system or environment commonly via random variables or fields, which is described by precise probability distribution functions based on the probabilistic theory. The later or subjective uncertainty represents incomplete or limited information for a physical system or environment often by intervals, evidence variables, probability-boxes and so on [29,30,31]. The majority of current studies with respect to uncertainty focus on either aleatory or epistemic uncertainty. However, it is noted that a number of engineering problems actually involve both types of uncertainties in the design [32]. Hence, this paper investigates the design optimization problems of structures under the hybrid uncertainties. For some uncertain parameters, we can obtain a sufficient number of high-quality samples to create their precise probability distributions, while for some other uncertain parameters, due to difficulties or high costs in testing, the interval bounds are relatively easier to be found. For example, the processing tolerance of a dimension parameter is based on the precision of the processing equipment, then it is easier to determine an interval for the actual dimension after processing based on the nominal design value and the tolerance. For another example, the loadings of a bridge or a building will be affected by the environment (e.g. wind, weather, temperature). Since there exist difficulties in testing to get large amounts of accumulated data due to the complexity of the environment, it will be relatively convenient if we model these parameters as intervals based on a limited number of samples. Recently engineering design problems with random-interval hybrid uncertainties have aroused great attentions [33,34,35,36,37,38,39].

For uncertainty analysis problems with both random and interval uncertainties, there is a challenging that the computational cost is relatively high and may even increase exponentially [40]. In order to improve the computational efficiency, some existing probability-interval uncertainty propagation analysis methods used the first-order or the second-order Taylor expansion to approximate the performance function. The first-order Taylor expansion cannot ensure a satisfactory accuracy especially for relatively large levels of uncertainties or nonlinearity problems. The second-order Taylor expansion generally has a better accuracy

than the first-order Taylor expansion, but the difficulty is the calculation of the second-order derivatives. Recently, a Polynomial Chaos-Chebyshev Interval (PCCI) method [41] was proposed to estimate the mean and variation bounds of the response. This method is effective, but the issue is still the computational cost that will increase exponentially with the increase of the uncertain variables. How to develop new and more efficient random-interval hybrid uncertainty propagation analysis methods is of great significance in engineering. The univariate dimension reduction method, which has a good global approximation performance, has been proven to be effective for uncertainty propagation analysis [42,43]. However, this paper should be the first study to introduce the dimension reduction method to uncertainty analysis and design problems under hybrid uncertainties.

Uncertainties can be incorporated into topological optimization to formulate the reliability-based topology optimization (RBTO) or robust topology optimization (RTO) [44,45]. In RBTO problems, the optimization model is generally formulated with reliability constraints to account for uncertainties [46,47], such as materials and loading uncertainties using probabilistic methods [48,49]. Du and Sun [50] developed a reliability-based topology optimization method for vibro-acoustic problems with probability uncertainties to obtain the optimal periodically arranged microstructures. For RTO problems, the optimization model usually aims to minimize both the mean and variance of the uncertain objective function [51,52,53,54]. Interval uncertainties have also been considered in structural topology optimization problems, such as the ellipsoid-based models [55,56,57]. For example, Guo et al [58] investigated the robust concurrent topology optimization with load uncertainties by the ellipsoid model. Recently, there have also been a few works for topology optimization considering hybrid uncertainties. For instance, Wu et al [59] introduced random-interval uncertainties into robust topological design of microstructures for mechanical metamaterials by using the PCCI method [41]. In [60], the hybrid stochastic interval perturbation method is used to develop a robust topology optimization method for structures. As aforementioned, the random-interval hybrid uncertainties have seldom been applied to the concurrent topological design of material microstructure and composite macrostructure.

In this paper, a new hybrid univariate dimension reduction (HUDR) method is proposed to estimate the interval mean and interval variance of the uncertain objective function by combining the dimension-reduction method with the random-interval model for hybrid uncertainty analysis. For problems with both random and interval hybrid uncertainties, the computational cost may increase exponentially, because each combination of interval values requires one probabilistic analysis. Furthermore, the integrated design of topology optimization for continuum structures itself is a cost-expensive numerical iterative procedure, so the computation for topology optimization problems under the hybrid uncertainties is sometimes computationally prohibitive. HUDR can efficiently provide accurate estimations of the statistic moments,

and the robust optimization model is constructed under the worst case for the existence of interval variables to avoid a double loop procedure for the large-scale topology optimization.

## 2. Deterministic multi-scale topology optimization

### 2.1 Problem statement

In this work, multi-scale topology optimization is conducted to find the material layout for a structure in both macro and micro scales to minimize the compliance under constraints. The macrostructure is assumed to be constructed by periodical microstructures to improve the possibility of practical applications. The optimization formulation is constructed based on the so called PAMP multi-scale optimization model in [23]. There are two materials involved in this study, the base material and the composite material. The material microstructure is assumed to be made of the base material and the macrostructure is assumed to be made of periodic microstructures.

The process for the multi-scale topology optimization is illustrated in Fig.1. The macrostructure A is periodically composed of the microstructure C. In the concurrent design optimization, the macrostructure material distribution and the material microstructure can be simultaneously optimized, thus providing more design flexibilities in order to minimize the compliance of the structure. As shown in Fig. 1, there are two coordinate systems, the global macro-coordinate  $X$  and the local micro-coordinate  $Y$ . The size of the microstructure is assumed to be small enough compared with the dimension of the macrostructure, and the microstructure is supposed to have the periodicity. In this case, the material properties at macro level can be calculated by the numerical homogenization method [1].

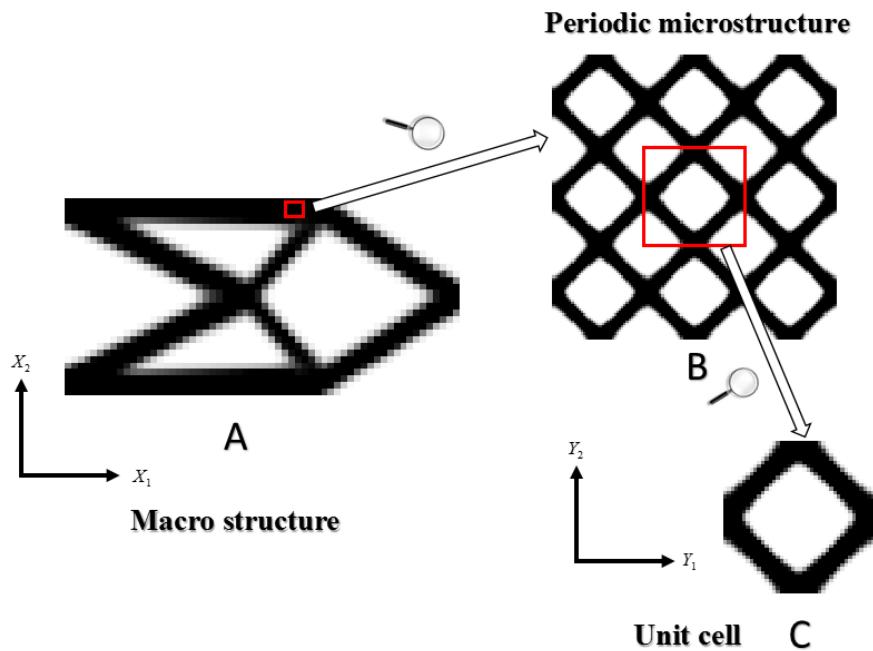


Fig.1 Schematic diagram of multi-scale topology optimization process

## 2.2 Mathematical formulation for deterministic design problem

Macro structural design and micro material design are combined into one system by using the homogenization theory. The concurrent design for both levels generally includes a two-stage coupled process: the outer stage is topology optimization for macrostructure to obtain the best layout for the macro structure, and the inner stage is topology optimization for the microstructure to optimize the unit cell and obtain the effective elastic matrix. Design variables in the macro scale are the relative densities of elements to discretize the macro design domain, and design variables in the micro scale are the relative densities of elements used to discretize the micro unit cell. The mathematical formulation is given as follows:

$$\begin{aligned}
\min_{\alpha_i, \rho_e} C(\alpha_i, \rho_e) &= \mathbf{U}(\alpha_i, \rho_e)^T \mathbf{K}(\alpha_i, \rho_e) \mathbf{U}(\alpha_i, \rho_e) \\
&= \sum_{i=1}^M (\alpha_i)^p \mathbf{U}_i^T \mathbf{K}^H(\rho_e) \mathbf{U}_i \\
st. \quad &\mathbf{K}(\alpha_i, \rho_e) \mathbf{U}(\alpha_i, \rho_e) = \mathbf{F} \\
&\sum_{i=1}^M \alpha_i V_i \leq f_1 V, \sum_{e=1}^N \rho_e V_e^i \leq f_2 V_i \\
&\alpha_{\min} \leq \alpha_i \leq 1, \rho_{\min} \leq \rho_e \leq 1 \\
&(i = 1, 2, \dots, M ; e = 1, 2, \dots, N)
\end{aligned} \tag{1}$$

in which  $C$  represents the compliance of the macrostructure,  $\alpha_i (i = 1, 2, \dots, M)$  and  $\rho_e (e = 1, 2, \dots, N)$  are the design variables (relative densities) of the  $i$ th and  $e$ th elements of the macrostructure and microstructure, respectively,  $M$  and  $N$  are the numbers of macro finite element and micro finite element respectively.  $p$  is the exponent of penalization ( $p = 3$  is used in this paper).  $\mathbf{U}$  and  $\mathbf{U}_i$  denote the global and elemental displacement matrix of the macrostructure.  $\mathbf{K}$  denotes the global stiffness matrix, and  $\mathbf{K}^H$  denotes the homogenized stiffness matrix of a macro element whose artificial density is equal to 1.  $\mathbf{F}$  is the external force of the structure.  $V$  and  $V_i$  represent the volume of the macrostructure and the unit cell, and  $V_e^i$  represents the element volume of the unit cell.  $f_1$  and  $f_2$  are volume fractions for volume constraints.  $\alpha_{\min}$  and  $\rho_{\min}$  are the minimum element relative densities to avoid singularity in numerical implementation.

Eq. (1) is a concurrent topology optimization problem and we can see that the objective function depends on both the macro design variable  $\alpha_i$  and the micro design variable  $\rho_e$ . The material interpolation schemes should be employed in both scales to obtain clear topologies. In the micro scale, the element elastic matrix can be expressed as:

$$\mathbf{D}(\rho_e) = (\rho_e)^p \mathbf{D}^0 \tag{2}$$

in which  $\mathbf{D}^0$  is the elastic matrix of the solid material. In the macro scale, the element elastic matrix  $\mathbf{D}^M$  is:

$$\mathbf{D}^M(\alpha_i, \rho_e) = (\alpha_i)^p \mathbf{D}^H(\rho_e) \quad (3)$$

In order to obtain the objective function value, the finite element analysis in the macro scale is formulated to get the global displacement  $\mathbf{U}$ . The global stiffness matrix  $\mathbf{K}$  can be calculated by assembling the elemental stiffness matrix  $\mathbf{K}_i$ , and  $\mathbf{K}_i$  can be obtained by:

$$\mathbf{K}_i(\alpha_i, \rho_e) = \int_{V_i} \mathbf{B} \mathbf{D}^M(\alpha_i, \rho_e) \mathbf{B} dV_i = (\alpha_i)^p \mathbf{K}^H(\rho_e) \quad (4)$$

$\mathbf{K}^H$  can be calculated as follows:

$$\mathbf{K}^H(\rho_e) = \int_{V_i} \mathbf{B} \mathbf{D}^H(\rho_e) \mathbf{B} dV_i \quad (5)$$

where  $\mathbf{B}$  is the strain-displacement matrix,  $\mathbf{D}^H$  denotes the effective elastic matrix of the microstructure, and can be obtained in the micro scale using the homogenization method [61,62,63]:

$$\mathbf{D}^H(\rho_e) = \frac{1}{|V_i|} \int_{V_i} (\mathbf{I} - \mathbf{b} \chi_i)^T \mathbf{D}(\rho_e) (\mathbf{I} - \mathbf{b} \chi_i) dV_i \quad (6)$$

in which  $\mathbf{I}$  is a three times three identity matrix in 2D (six in 3D), corresponding to the applied unit strain fields that include the horizontal unit strain, the vertical unit strain and the shear unit strain.  $\chi_i$  is the nodal displacement field of the microstructure by globally enforcing the unit strain fields, and  $\mathbf{b}$  is the strain-displacement matrix. The finite element analysis in the micro scale subjected to the periodic boundary conditions is formulated as follows:

$$\mathbf{k} \chi_i = \mathbf{f} \quad (7)$$

where

$$\mathbf{k} = \int_{V_i} \mathbf{b}^T \mathbf{D}(\rho_e) \mathbf{b} dV_i \quad (8)$$

$$\mathbf{f} = \int_{V_i} \mathbf{b}^T \mathbf{D}(\rho_e) dV_i \quad (9)$$

After calculating the stiffness matrix  $\mathbf{k}$  of the microstructure and the force  $\mathbf{f}$  corresponding to unit strain fields, we can get the microstructural displacement field  $\chi_i$ . Then the homogenized constitutive matrix  $\mathbf{D}^H$  can be computed by Eq. (6).

Sensitivities of the objective function with respect to the design variables are required to guide the optimization direction during the iteration process. In the macro scale, the sensitivities of the objective function with respect to  $\alpha_i$  can be expressed by the adjoint variable method [64]:

$$\frac{\partial C}{\partial \alpha_i} = -\mathbf{U}^T \frac{\partial \mathbf{K}(\alpha_i, \rho_e)}{\partial \alpha_i} \mathbf{U} = -p(\alpha_i)^{p-1} \mathbf{U}_i^T \mathbf{K}^H(\rho_e) \mathbf{U}_i \quad (10)$$

In the micro scale, the sensitivities of the objective function with respect to  $\rho_e$  are equal to the summation of sensitivities of all macro elements compliance with respect to  $\rho_e$ :



$$\frac{\partial C}{\partial \rho_e} = -\mathbf{U}^T \frac{\partial \mathbf{K}(\alpha_i, \rho_e)}{\partial \rho_e} \mathbf{U} = -\sum_{i=1}^M (\alpha_i)^p \mathbf{U}_i^T \left( \int_{V_i} \mathbf{B}^T \frac{\partial \mathbf{D}^H(\rho_e)}{\partial \rho_e} \mathbf{B} dV_i \right) \mathbf{U}_i \quad (11)$$

Based on (6), the derivative of  $\mathbf{D}^H$  with respect to  $\rho_e$  can be obtained from:

$$\frac{\partial \mathbf{D}^H(\rho_e)}{\partial \rho_e} = \frac{1}{|V_i|} \int_{V_i} (\mathbf{I} - \mathbf{b}\chi_i)^T \frac{\partial \mathbf{D}(\rho_e)}{\partial \rho_e} (\mathbf{I} - \mathbf{b}\chi_i) dV_i = \frac{1}{|V_i|} \int_{V_i} (\mathbf{I} - \mathbf{b}\chi_i)^T \left( p(\rho_e)^{p-1} \mathbf{D}^0 \right) (\mathbf{I} - \mathbf{b}\chi_i) dV_i \quad (12)$$

Then the sensitivities of the objective function with respect to  $\rho_e$  can be found by:

$$\frac{\partial C}{\partial \rho_e} = -\mathbf{U}^T \frac{\partial \mathbf{K}(\alpha_i, \rho_e)}{\partial \rho_e} \mathbf{U} = -\frac{1}{|V_i|} \sum_{i=1}^M (\alpha_i)^p \mathbf{U}_i^T \left( \int_{V_i} \mathbf{B}^T \left[ \int_{V_i} (\mathbf{I} - \mathbf{b}\chi_i)^T \left( p(\rho_e)^{p-1} \mathbf{D}^0 \right) (\mathbf{I} - \mathbf{b}\chi_i) dV_i \right] \mathbf{B} dV_i \right) \mathbf{U}_i \quad (13)$$

From the above, we can see that the designs in both scales (the outer and the inner scales) are coupled. The displacement field of the macrostructure is needed to evaluate the sensitivities with respect to the micro design variables in the inner stage, and the effective elastic tensor obtained from the micro scale calculation is used as the material property for the macrostructure in the outer stage.

### 3. Robust topology optimization under hybrid uncertainties

#### 3.1 Mathematical formulation for RTO

Assume  $\mathbf{X} = (X_1, X_2, \dots, X_n)$  is the probability vector and  $\mathbf{Y} = (Y_1, Y_2, \dots, Y_h)$  is the interval vector in the structure.  $X_i (i=1, 2, \dots, n)$  is the  $i$ th probability uncertain variable and the probability distribution function is given as  $f_{X_i}(X_i)$ .  $Y_i (i=1, 2, \dots, h)$  is the  $i$ th interval variable, and the interval variation of the interval variable is given as  $[Y_i^L, Y_i^R]$ .  $Y_i^C = \frac{Y_i^L + Y_i^R}{2}$  and  $Y_i^W = \frac{Y_i^R - Y_i^L}{2}$  represent the interval midpoint and the interval radius of  $Y_i$ , respectively.

With probability and interval variables, the optimization problem can be rewritten as:

$$\begin{aligned} \min_{\alpha_i, \rho_e} C(\mathbf{X}, \mathbf{Y}) &= \mathbf{U}^T \mathbf{K} \mathbf{U} = \sum_{i=1}^M (\alpha_i)^p \mathbf{U}_i^T(\mathbf{X}, \mathbf{Y}) \mathbf{K}^H \mathbf{U}_i(\mathbf{X}, \mathbf{Y}) \\ \text{st.} \quad &\mathbf{K}(\mathbf{X}, \mathbf{Y}) \mathbf{U}(\mathbf{X}, \mathbf{Y}) = \mathbf{F}(\mathbf{X}, \mathbf{Y}) \\ &\sum_{i=1}^M \alpha_i V_i \leq f_1 V, \sum_{e=1}^N \rho_e V_e^i \leq f_2 V_i \\ &\alpha_{\min} \leq \alpha_i \leq 1, \rho_{\min} \leq \rho_e \leq 1 \end{aligned} \quad (14)$$

The compliance  $C$  illustrates the stiffness of the structure, and it is known that smaller compliance means stiffer structure. The robust objective function is defined as a linear combination of the mean and standard deviation of structure compliance due to the probabilistic and interval variables. The robust topology optimization can be reformulated under the worst case:

$$\begin{aligned}
\min_{\alpha_i, \rho_e} g &= \max_{\mathbf{Y}} \mu(C) + w \cdot \sigma(C) \\
st. \quad &\mathbf{K}(\mathbf{X}, \mathbf{Y})\mathbf{U}(\mathbf{X}, \mathbf{Y}) = \mathbf{F}(\mathbf{X}, \mathbf{Y}) \\
&\sum_{i=1}^M \alpha_i V_i \leq f_1 V, \sum_{e=1}^N \rho_e V_e^i \leq f_2 V_i \\
&\alpha_{\min} \leq \alpha_i \leq 1, \rho_{\min} \leq \rho_e \leq 1
\end{aligned} \tag{15}$$

where  $\mu(C) = E(C)$  represents the mean value of the compliance.  $\sigma(C) = \left(E(C^2) - E^2(C)\right)^{\frac{1}{2}}$  is the standard deviation of compliance, where  $E(C^k), k=1,2$  denote the first and second origin moments of the structure compliance respectively, and  $w$  represents a given weight value.

### 3.2 Hybrid univariate dimension reduction method for RTO

During the optimization (15), a HUDR method is proposed for efficient structural analysis of hybrid uncertainties. For structure compliance  $C = C(\mathbf{X}, \mathbf{Y})$  with  $n$  probabilistic variables and  $h$  interval variables, the  $k$ th origin moment  $E(C^k)$  can be expressed as:

$$\begin{aligned}
E(C^k) &= E\left([C(\mathbf{X}, \mathbf{Y})]^k\right) = \int_{-\infty}^{\infty} \int_{-\infty}^{\infty} \dots \int_{-\infty}^{\infty} C^k(\mathbf{X}, \mathbf{Y}) f(X_1, X_2, \dots, X_n) dX_1 dX_2 \dots dX_n \\
&= \int_{-\infty}^{\infty} \int_{-\infty}^{\infty} \dots \int_{-\infty}^{\infty} C^k(\mathbf{X}, \mathbf{Y}) f(X_1) f(X_2) \dots f(X_n) dX_1 dX_2 \dots dX_n
\end{aligned} \tag{16}$$

where  $f(X_1, X_2, \dots, X_n)$  is the joint probability distribution function of the probability uncertain variables.

Firstly, we assume that interval variables are fixed, so the above equation becomes a multidimensional integral problem with probabilistic uncertainties. By the univariate dimension reduction method [42], the multidimensional problem will be transformed into a series of one-dimensional problems. As a result, the multidimensional Gauss integral is changed to a one-dimensional Gauss integral. By introducing the univariate dimension reduction technique, the compliance can be approximated as follows:

$$C(\mathbf{X}, \mathbf{Y}) \cong \sum_{j=1}^n \hat{C}_j(\mathbf{X}, \mathbf{Y}) - (n-1)C(u_1, u_2, \dots, u_n) \tag{17}$$

where  $\hat{C}_j(\mathbf{X}, \mathbf{Y}) = C(u_1, \dots, u_{j-1}, X_j, u_{j+1}, \dots, u_n)$ ,  $u_j$  is the mean value of  $X_j$ . Then the  $k$ th origin moment of the compliance is given by:

$$E(C^k) = E\left(\left[\sum_{j=1}^n \hat{C}_j(\mathbf{X}, \mathbf{Y}) - (n-1)C(u_1, u_2, \dots, u_n)\right]^k\right) \tag{18}$$

Based on the binomial theorem, we can obtain:

$$E(C^k) = \sum_{i=0}^k \binom{k}{i} E\left(\sum_{j=1}^n \hat{C}_j(\mathbf{X}, \mathbf{Y})\right)^i \left[-(n-1)C(u_1, u_2, \dots, u_n)\right]^{k-i} \tag{19}$$

in which  $\binom{k}{i} = \frac{k!}{i!(k-i)!}$  is the binomial expansion coefficient. Define:

$$S_j^i = E \left[ \left\{ \sum_{i=1}^j \hat{C}_j(\mathbf{X}, \mathbf{Y}) \right\}^i \right] \quad (20)$$

in which  $j=1, \dots, n$ ;  $i=1, \dots, k$ .  $S_j^i$  can be calculated by the following recursion formula:

$$\begin{aligned} S_1^i &= E \left[ \left( \hat{C}_1(\mathbf{X}, \mathbf{Y}) \right)^i \right]; & i=1, \dots, k \\ S_2^i &= \sum_{l=0}^i \binom{i}{l} S_1^l E \left[ \left( \hat{C}_2(\mathbf{X}, \mathbf{Y}) \right)^{i-l} \right]; & i=1, \dots, k \\ &\vdots \\ S_j^i &= \sum_{l=0}^i \binom{i}{l} S_{j-1}^l E \left[ \left( \hat{C}_j(\mathbf{X}, \mathbf{Y}) \right)^{i-l} \right]; & i=1, \dots, k \\ &\vdots \\ S_n^i &= \sum_{l=0}^i \binom{i}{l} S_{n-1}^l E \left[ \left( \hat{C}_n(\mathbf{X}, \mathbf{Y}) \right)^{i-l} \right]; & i=1, \dots, k \end{aligned} \quad (21)$$

Then

$$E(C^k(\mathbf{Y})) = \sum_{i=0}^k \binom{k}{i} S_n^i \left[ -(n-1)C(u_1, u_2, \dots, u_n) \right]^{k-i} \quad (22)$$

From the above we can see that the origin moments of the system can be calculated from the origin moments of subsystems with single variable. For random variables with normal distributions, the first and second moments of the univariate function  $\hat{C}_j(\mathbf{X}, \mathbf{Y})$  are obtained by using Gauss-Hermite numerical integral. For random variables with other distributions, we can firstly transform the variables into normal distributions through a probability transformation [65], and then calculate the first and second moments by using Gauss-Hermite numerical integral. For simplicity but without losing any generality, in this paper we assume the random variables under normal distributions.

After that, if we take interval variables into consideration, the  $k$ th statistic matrix of the system calculated from Equation (22) will becomes an interval rather than a single value:

$$E(C^k(\mathbf{Y})) = [\min_{\mathbf{Y}} E(C^k(\mathbf{Y})), \max_{\mathbf{Y}} E(C^k(\mathbf{Y}))] \quad (23)$$

Then the objective function of the robust topology optimization problem (15) only contains interval variables. Similarly, the objective function can be approximated as:

$$\begin{aligned}
g &= \max_Y \mu(C(Y_1, Y_2, \dots, Y_h)) + w \cdot \sigma(C(Y_1, Y_2, \dots, Y_h)) \\
&\cong \max_Y \mu(C(Y_1, Y_2^C, \dots, Y_h^C)) + \mu(C(Y_1^C, Y_2, \dots, Y_h^C)) + \dots \\
&\quad + \mu(C(Y_1^C, Y_2^C, \dots, Y_h)) - (h-1) \cdot \mu(C(Y_1^C, Y_2^C, \dots, Y_h^C)) \\
&\quad + w \cdot \sigma(C(Y_1, Y_2^C, \dots, Y_h^C)) + w \cdot \sigma(C(Y_1^C, Y_2, \dots, Y_h^C)) + \dots \\
&\quad + w \cdot \sigma(C(Y_1^C, Y_2^C, \dots, Y_h)) - (h-1) \cdot w \cdot \sigma(C(Y_1^C, Y_2^C, \dots, Y_h^C)) \\
&= \max_Y d_1(Y_1) + d_2(Y_2) + \dots + d_h(Y_h) - d_c
\end{aligned} \tag{24}$$

where

$$d_i(Y_i) = \mu(C(Y_1^C, \dots, Y_i, \dots, Y_h^C)) + w \cdot \sigma(C(Y_1^C, \dots, Y_i, \dots, Y_h^C)), i = 1, 2, \dots, h \tag{25}$$

$$d_c = (h-1) \cdot \mu(C(Y_1^C, Y_2^C, \dots, Y_h^C)) + (h-1) \cdot w \cdot \sigma(C(Y_1^C, Y_2^C, \dots, Y_h^C)) \tag{26}$$

From the above we can see that,  $d_i(Y_i)$  is a function with an interval variable  $Y_i$ , and  $d_c$  is a constant. Using the first order Taylor series:

$$d_i(Y_i) \cong d_i(Y_i^C) + \nabla d_i \cdot (Y_i - Y_i^C) \tag{27}$$

where  $\nabla d_i$  represents the sensitivity of  $d_i$  with respect to interval variable  $Y_i$ . In order to obtain the maximum value of  $d_i$ , we can get the corresponding interval value from the sign of the sensitivity of  $d_i$ : if  $\nabla d_i > 0, Y_i = Y_i^R$ ; if  $\nabla d_i < 0, Y_i = Y_i^L$ . As a result, the value of the objective function  $g = \max \mu(C) + w \cdot \sigma(C)$  can be obtained.

If we assume there are  $n$  random variables and  $h$  interval variables, by using the hybrid univariate dimension reduction method in this paper, only  $(3n+1) \times (2h+1)$  finite element analysis (FEA) calls are needed in the approximation of the performance function. Hence, the proposed uncertainty analysis method (HUDR) can greatly improve the computational efficiency in uncertainty analysis and robust topological design. For numerical accuracy of the proposed method, in the numerical examples, the robust objective function values are provided for both deterministic and uncertain topology optimization results. In order to validate the accuracy, the robust objective function values have also been calculated by using the Monte Carlo simulation (MCS). It can be seen that the results obtained by the proposed method in this paper are very close to the MCS results, which means the proposed method has a very good accuracy.

### 3.3 Sensitivity analysis

The sensitivities of the objective function with respect to the macro design variables can be calculated by:

$$\frac{\partial(\mu(C) + w \cdot \sigma(C))}{\partial \alpha_i} = \frac{\partial \mu(C)}{\partial \alpha_i} + w \cdot \frac{\partial \sigma(C)}{\partial \alpha_i} \tag{28}$$

Based on the compound function derivation law, we have:

$$\frac{\partial \sigma^2(C)}{\partial \alpha_i} = 2 \cdot \sigma(C) \cdot \frac{\partial \sigma(C)}{\partial \alpha_i} \tag{29}$$

Then Equation (28) will be changed to the following:

$$\begin{aligned}
\frac{\partial(\mu(C) + w \cdot \sigma(C))}{\partial \alpha_i} &= \frac{\partial \sum_{l=1}^L C_l / L}{\partial \alpha_i} + w \cdot \frac{\partial \sum_{l=1}^L (C_l - \mu(C))^2 / L}{2 \cdot \sigma(C) \cdot \partial \alpha_i} \\
&= \frac{\partial \sum_{l=1}^L C_l}{\partial \alpha_i} / L + 2w \cdot \sum_{l=1}^L |C_l - \mu(C)| \cdot \frac{\partial(C_l - \mu(C))}{2 \cdot \sigma(C) \cdot \partial \alpha_i} / L \\
&= \sum_{l=1}^L \frac{\partial C_l}{\partial \alpha_i} / L + \frac{w}{\sigma(C)} \cdot \sum_{l=1}^L |C_l - \mu(C)| \cdot \frac{\partial C_l}{\partial \alpha_i} / L
\end{aligned} \tag{30}$$

where  $C_l$  means the  $l$  th value of  $L$  samples of compliance values. From the above we can see that  $\left( \sum_{l=1}^L \partial C_l / \partial \alpha_i \right) / L$  is just the mean value of function  $\partial C / \partial \alpha_i$ , and  $\left( \sum_{l=1}^L |C_l - \mu(C)| \cdot (\partial C / \partial \alpha_i) \right) / L$  is just the mean value of function  $|C - \mu(C)| \cdot (\partial C / \partial \alpha_i)$ .

From Equation (10), the explicit expression of  $\partial C / \partial \alpha_i$  and  $|C - \mu(C)| \cdot (\partial C / \partial \alpha_i)$  can be obtained, and the mean value  $E(\partial C / \partial \alpha_i)$  and  $E(|C - \mu(C)| \cdot (\partial C / \partial \alpha_i))$  can be easily obtained using the same formula as Equation (22).

Similarly, the sensitivities of the objective function with respect to micro design variables are:

$$\frac{\partial(\mu(C) + w \cdot \sigma(C))}{\partial \rho_e} = \frac{\partial \mu(C)}{\partial \rho_e} + w \cdot \frac{\partial \sigma(C)}{\partial \rho_e} \tag{31}$$

In the same way, we will obtain:

$$\frac{\partial(\mu(C) + w \cdot \sigma(C))}{\partial \rho_e} = \sum_{l=1}^L \frac{\partial C_l}{\partial \rho_e} / L + \frac{w}{\sigma(C)} \cdot \sum_{l=1}^L |C_l - \mu(C)| \cdot \frac{\partial C_l}{\partial \rho_e} / L \tag{32}$$

Based on Equation (13), we can also easily obtain the sensitivities in (32). The Optimality Criteria (OC) method [66] is very efficient for optimization problems with a large number of design variables with single constraint, which is a typical case in the continuous shape and topology optimization with a material usage constraint. In this work, the OC method is used to update both macro and micro design variables in both scales. In order to obtain mesh-independent results, an efficient sensitivity filter proposed by Sigmund [67] is used in this work.

### 3.4 Optimization procedure

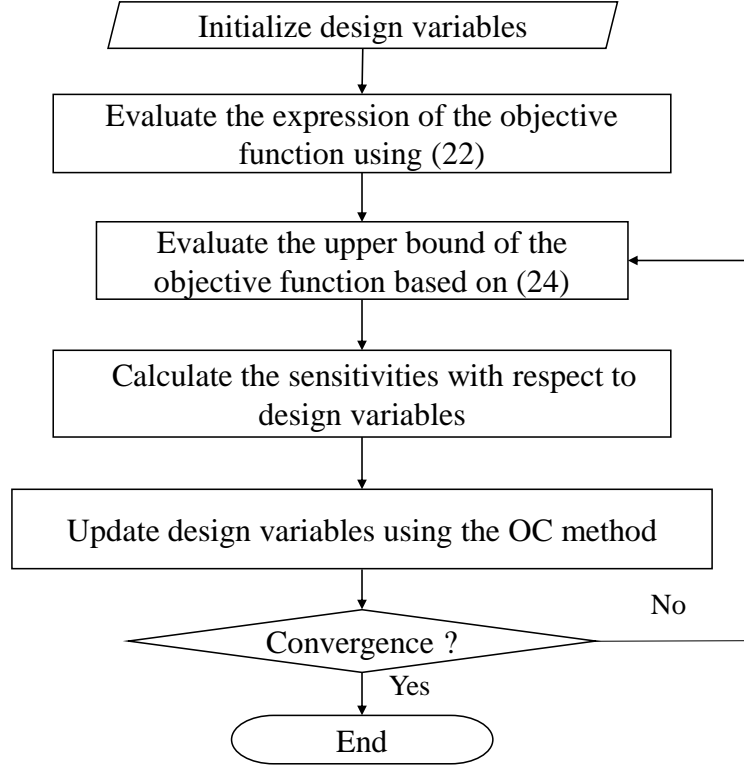


Fig.2 The flowchart of the proposed method

The process of the proposed multi-scale robust topology optimization method under hybrid uncertainties can be summarized as follows (Fig. 2):

- (1) Initialize the design variables  $\alpha_i$  and  $\rho_e$  in both scales;
- (2) Regarded the interval variables as constants, evaluate the expression of the objective function in (15) using equation (22);
- (3) Taken interval variation into consideration, evaluate the upper bound of the objective function based on equation (24);
- (4) Compute the sensitivities of the objective function with respect to design variables based on equations (30) and (32);
- (5) Update the macro and micro design variables using the OC method;
- (6) Check convergence. The convergence criterion is  $|g_m - g_{m-1}| / \max(g_m, g_{m-1}) \leq \varepsilon_{\max}$ .  $m$  is the current iteration step number, and  $\varepsilon_{\max}$  is set to be  $10^{-5}$ . If it is not convergent, go back to step (2); if it is, stop the iteration process.

#### 4. Numerical examples

In this part, three numerical examples are used to illustrate the effectiveness of the proposed method. In these examples, the macrostructure and the microstructure which is the same over all the domain are optimized concurrently. The macrostructure and the microstructure are discretized by using quadrilateral

elements with four nodes. The magnitudes of the applied loads are assumed as random variables and the loading directions are assumed to be interval variables. Considering the hybrid uncertainties, the proposed HUDR method is employed to obtain robust design results for structures. The weight  $w$  is set to be 1 in this paper, which means optimizing the mean performance is equally important as minimizing the standard deviation. The deterministic optimization results can be obtained for comparison, by using the mean values of the random variables and the central point values of the interval variables. The initial values for macro design variables  $\alpha_i$  are set to be 0.5. We have chosen a design with a hole at the central as the initial guess for microscopic design because a uniform initial design will make it difficult to solve material design problems using the numerical homogenization method [61]. The initial design of the micro unit cell is shown in Fig.3, in which the black colour represents solid material with artificial density 1, while the white area represents weak material with artificial density 0.001.

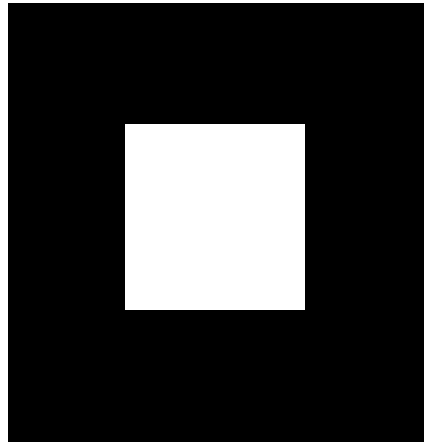


Fig.3 The initial design of the microstructure

#### 4.1 Cantilever beam

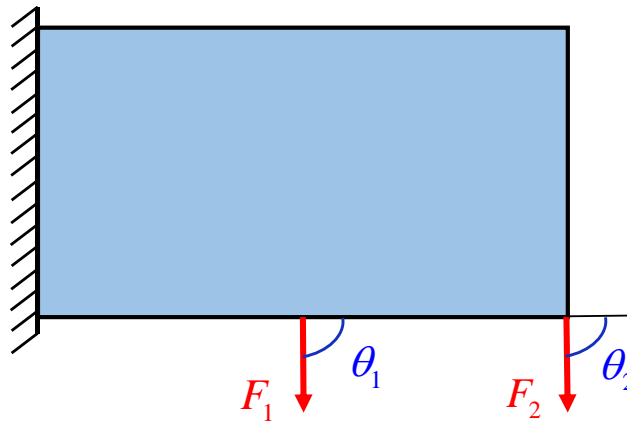


Fig.4 Cantilever beam

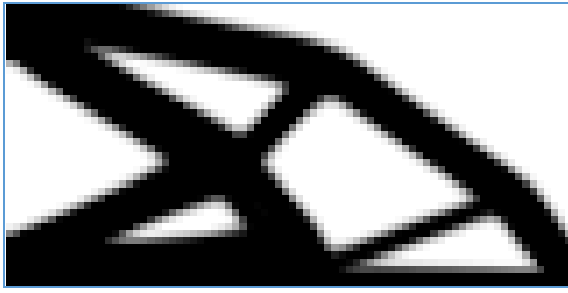
Consider a 2:1 (length: width) cantilever beam, the boundary conditions and loads are given in Fig.4. The elastic tensor for the artificial material is  $E=1$  and the Poisson's ratio is  $\nu=0.3$ . Two vertical loads  $F_1$  and  $F_2$  are applied on the middle point of the lower bound and the lower-right corner of the beam. In this example,

the loads  $F_1 \sim N(1, 0.1^2)$  and  $F_2 \sim N(1, 0.1^2)$  are both assumed as normal random variables, while the directions of the loads  $\theta_1 = [80^\circ, 100^\circ]$  and  $\theta_2 = [80^\circ, 100^\circ]$  are regarded as interval variables. The mesh size for the macrostructure is 80 by 40, and the mesh size for the microstructure is 40 by 40. The volume fractions for both macrostructure and microstructure are set as 0.5. This optimization problem is to minimize the compliance of the cantilever beam, so as to find the optimized topologies in both macro and micro scales under interval and random hybrid uncertainties.

As shown in Fig.5, a(1)~a(4) are results of the deterministic design, and b(1)~b(4) are results of the robust design. In Fig.5, the first four pictures are results in the macro scale: a(1) and b(1) are the final topologies of the macro structure, while a(2) and b(2) give the contour plots for the macro design. The last four pictures are results in the micro scale: a(3) and b(3) show the individual unit cells, while a(4) and b(4) are three by three arrays of the identical unit cells. It can be seen that the final topologies for the structure with uncertainties are different from the deterministic ones at both scales.

For comparison and verification purpose, the effective elastic matrices, the robust objective function values (including the mean and standard variance) and the FEA calls of the robust and the deterministic designs under the uncertain loads are given in Table 1. The effective elastic matrices show that the microstructure in the robust design has better resistance to externally applied forces from different directions than the deterministic design. When applying the uncertain loads to both deterministic and uncertain designs, we can obtain the robust objective function values 715.5839 and 657.0068, respectively, which indicate that the robust design can result in a smaller or better objective function value. For the given uncertain loads, the mean and the standard deviation of the robust design (569.2122 and 87.7946 respectively) are both much smaller than those of the deterministic design (619.7488 and 95.8351 respectively). It shows that the robust topology optimization considering uncertainties can provide a design with better robustness compared with the deterministic one. To verify the accuracy,  $10^7$  Monte Carlo simulations are used as references. It can be seen that the results obtained by our proposed method are close to the MCS results, and at the same time, the proposed method only need a small number of FEA calls. To evaluate the value of the robust objective function, the proposed method only needs 35  $((3 \times 2 + 1) \times (2 \times 2 + 1))$  FEA calls, but remains a very good accuracy. The iteration histories of both objective function and volume constraints as given in Fig. 6 show that the proposed method has good computational efficiency and stability.

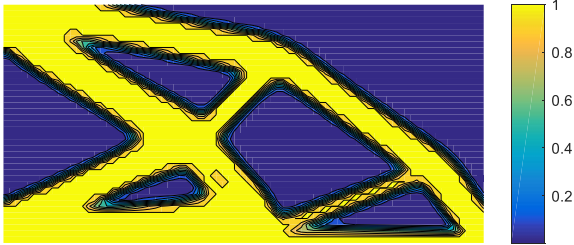




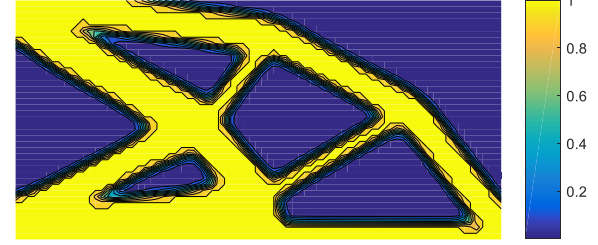
a(1)



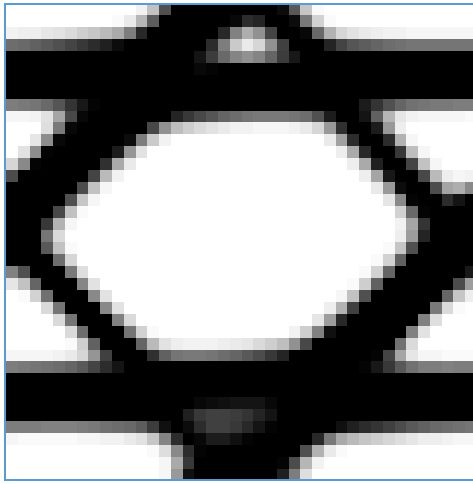
b(1)



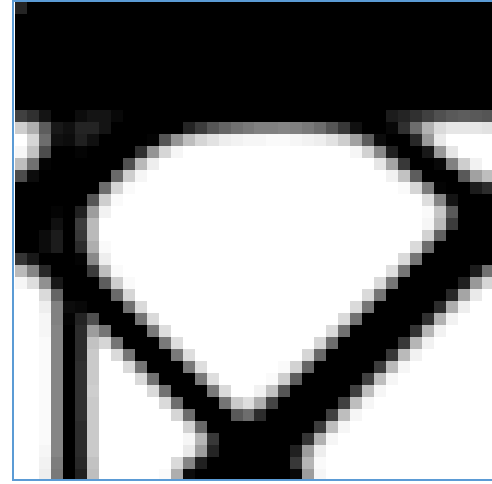
a(2)



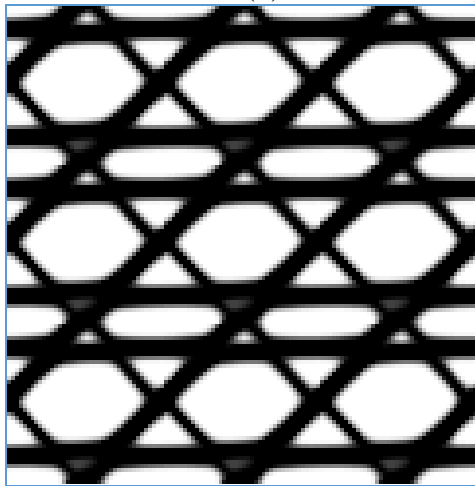
b(2)



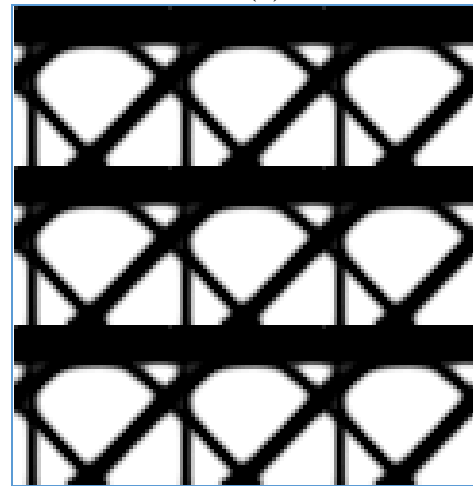
a(3)



b(3)

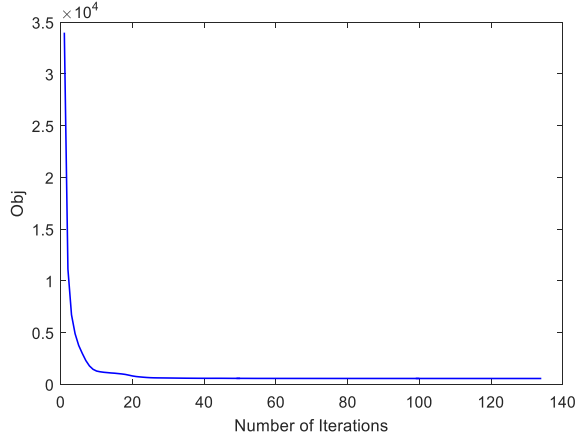


a(4)

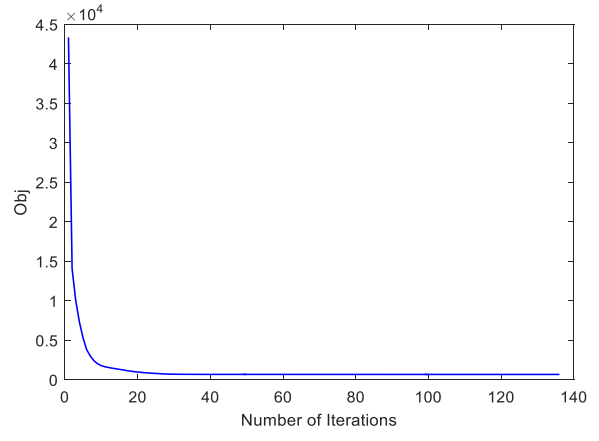


b(4)

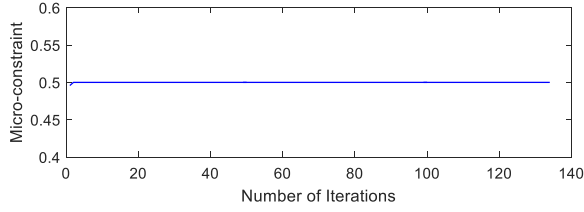
Fig. 5 Optimized results in macro and micro scales for cantilever beam  
(left: deterministic design; right: uncertain design)



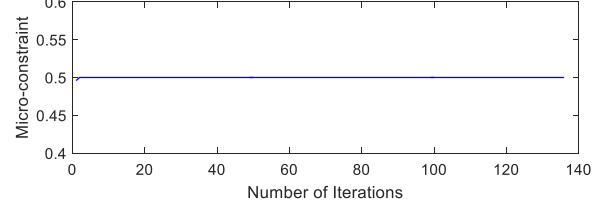
a(1)



b(1)



a(2)



b(2)

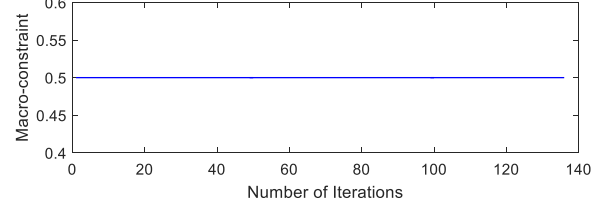
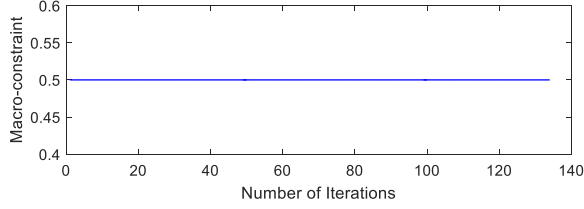


Fig. 6 Convergent history for cantilever beam  
(left: deterministic design; right: uncertain design)

#### 4.2 Messerschmitt-Bölkow-Blohm (MBB) beam

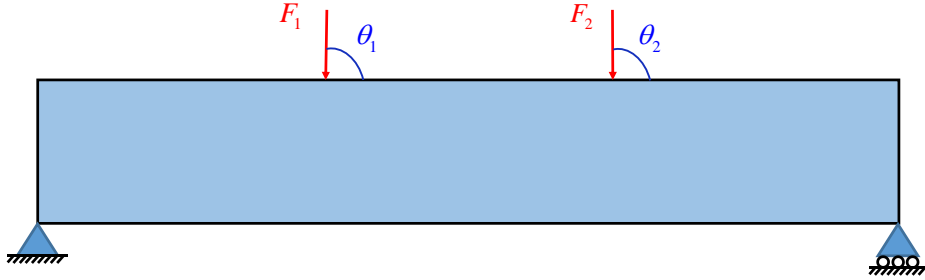
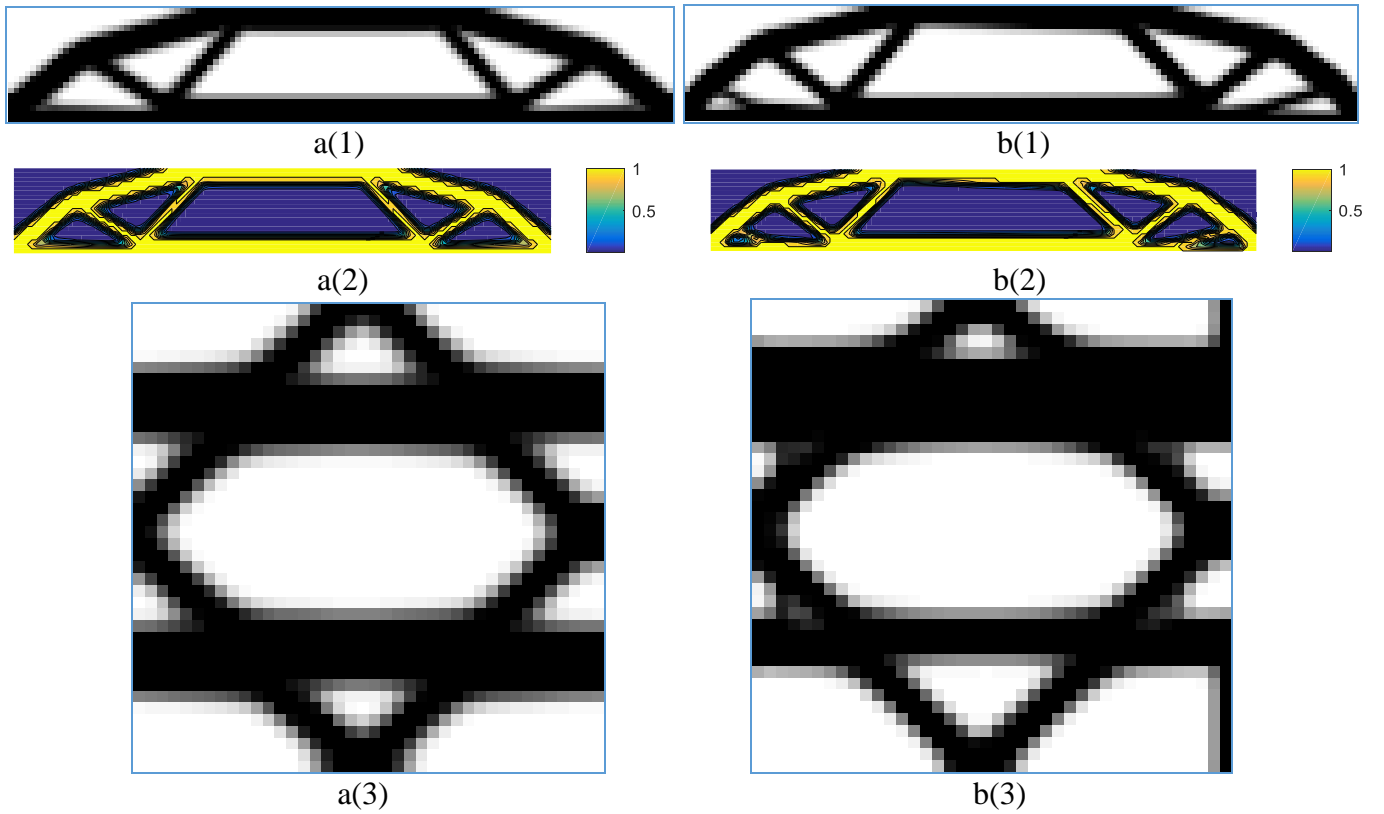


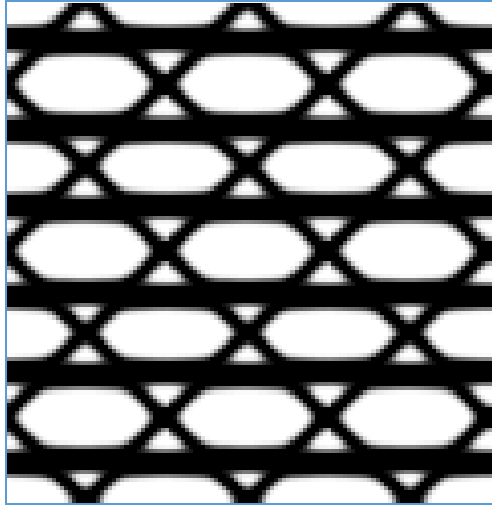
Fig.7 MBB beam

As shown in Fig.7 , the length-width ratio for the MBB beam is 6:1, and the lower left corner of the beam is clamped and the lower right corner is simply supported. Two external loads  $F_1$  and  $F_2$  are applied on the upper bound of the MBB beam. The magnitudes of the loads  $F_1 \sim N(1, 0.1^2)$  and  $F_2 \sim N(1, 0.1^2)$  are supposed to be normal random variables, and the directions of the loads  $\theta_1 = [80^\circ, 100^\circ]$  and  $\theta_2 = [80^\circ, 100^\circ]$  are regarded as interval variables. The elastic tensor and the Poisson's ratio for the artificial material are  $E=1$  and  $\nu=0.3$ .

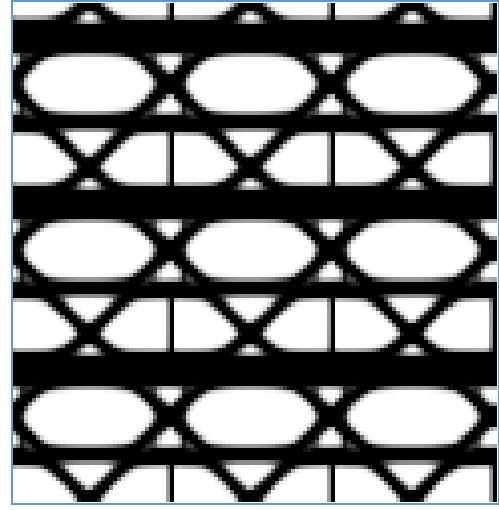
The mesh size for the macrostructure is 120 by 20, and the mesh size for the microstructure is 40 by 40. The volume fractions for both macrostructure and microstructure are 0.5.

Fig.8 gives the optimized results in the macro and micro scales for the MBB beam. It can be seen that the topological results for the structure with uncertainties are different from the deterministic ones. The corresponding effective elastic matrices and the robust objective function values for both deterministic and uncertain designs are shown in Table 2. Under the same uncertain loads, the robust objective function value for the deterministic design is  $1.3465e3$ , which is 8.7% larger than the robust objective function value for the robust design. It can be found that the topology optimization considering uncertainties provides more robust results than the deterministic topology optimization. The results by  $10^7$  Monte Carlo simulations are also provided to verify the accuracy of the proposed method. It can be seen that the results obtained by the proposed method have very good accuracy. The results denote that uncertainties may have obvious influence on the optimization results, so it is important and essential to consider uncertainties during the topological design process. The convergence histories of the objective function and volume constraints in Fig.9 indicate that the proposed method can obtain the optimization designs efficiently.



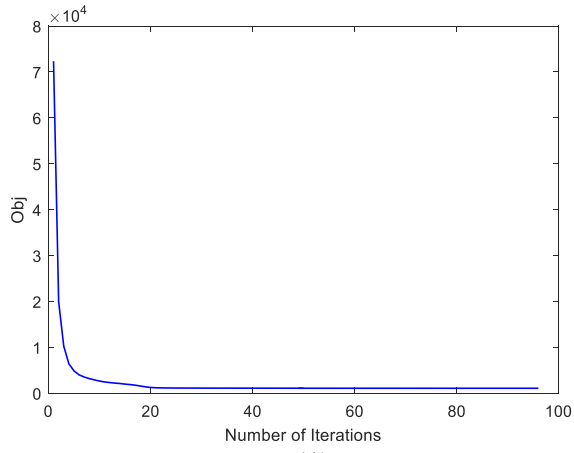


a(4)

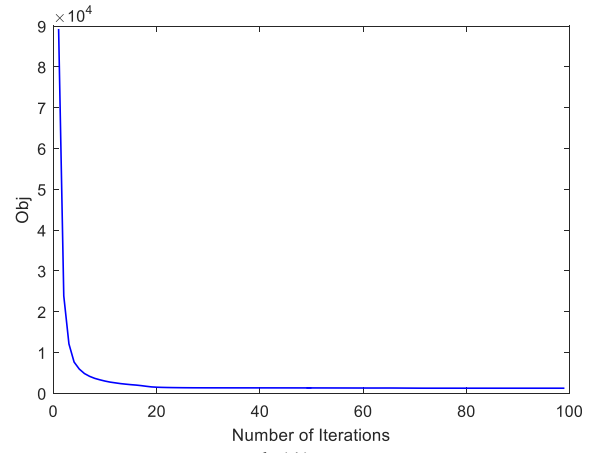


b(4)

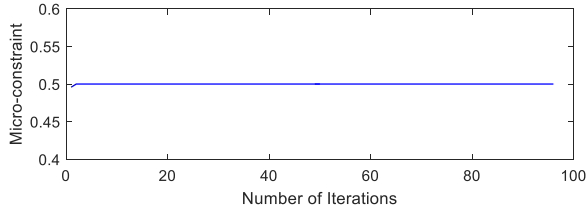
Fig. 8 Optimized results in macro and micro scales for MBB beam  
(left: deterministic design; right: uncertain design)



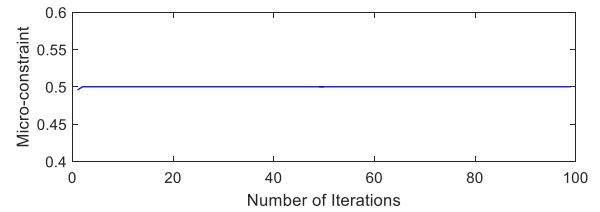
a(1)



b(1)



a(2)



b(2)

Fig. 9 Convergent history for MBB beam  
(left: deterministic design; right: uncertain design)

### 4.3 Michelle-type structure

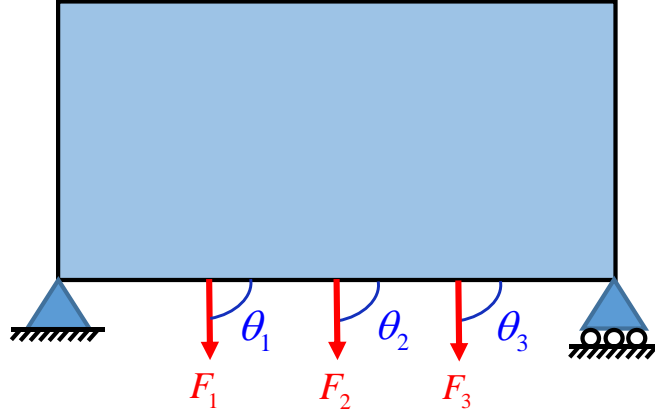


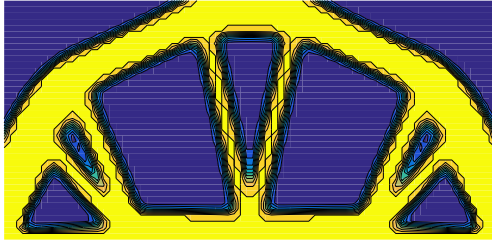
Fig. 10 Michelle-type structure

A Michelle structure with a 2:1 length-width ratio is investigated in this example. As shown in Fig.10, three external loads  $F_1$ ,  $F_2$  and  $F_3$  are vertically applied on the lower side of the structure. The lower left corner of the beam is clamped and the lower right corner is simply supported. The elastic tensor for the artificial material is  $E=1$  and its Poisson's ratio is  $\nu=0.3$ . The three loads  $F_1$ ,  $F_2$  and  $F_3$  are assumed as normal variables with mean values  $[1, 1, 1]$  and standard variances  $[0.1, 0.1, 0.1]$ , and the loads directions  $\theta_1$ ,  $\theta_2$ , and  $\theta_3$  are within intervals  $[80^\circ, 100^\circ]$ . The mesh size for the macrostructure is 80 by 40, and the mesh size for the microstructure is 40 by 40. The volume fractions for both macrostructure and microstructure are 0.5.

The optimized results for the Michelle-type structure with uncertainties are given in Fig. 11. Robust macro structure design in Fig. 11 b(1) is different from the deterministic macro design in a(1), although they have similar topologies. The robust microstructure design in b(3) is obviously different from the deterministic micro design in a(3). Table 3 gives the corresponding effective elastic matrices and the robust objective function values for both the deterministic and uncertain designs under the same uncertain loads. The robust objective function value for the deterministic design is 566.3863, and the robust objective function value for the robust design is 516.9915. It can be seen that the robust topology optimization provides better designs than the deterministic optimization. As a reference, the results by  $10^7$  Monte Carlo simulations are also provided. The convergent histories of the objective function and volume constraints are plotted in Fig.12.

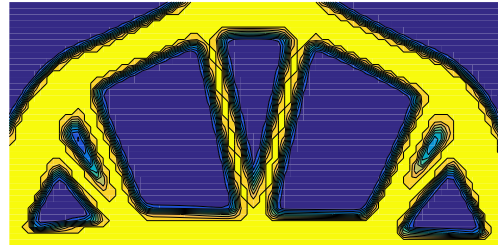


a(1)

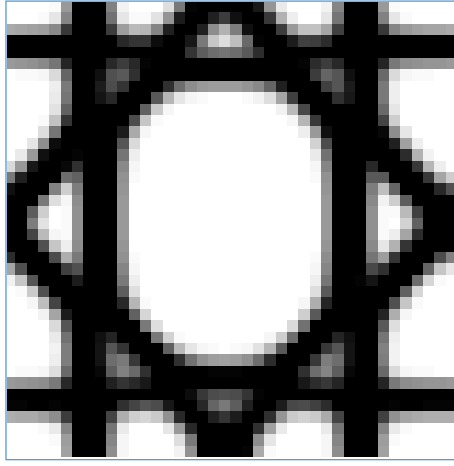


a(2)

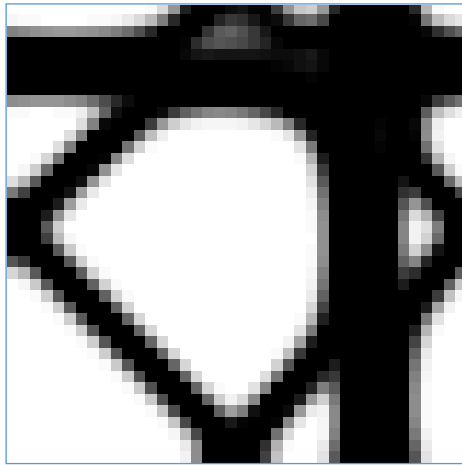
b(1)



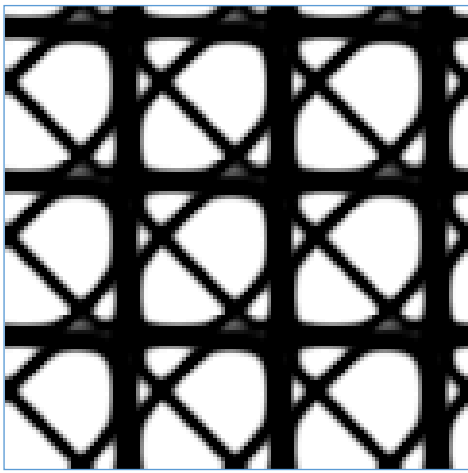
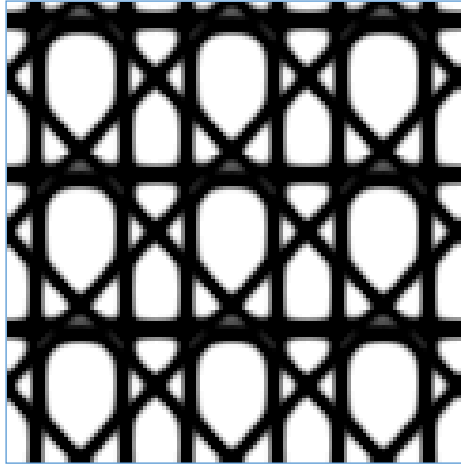
b(2)



a(3)



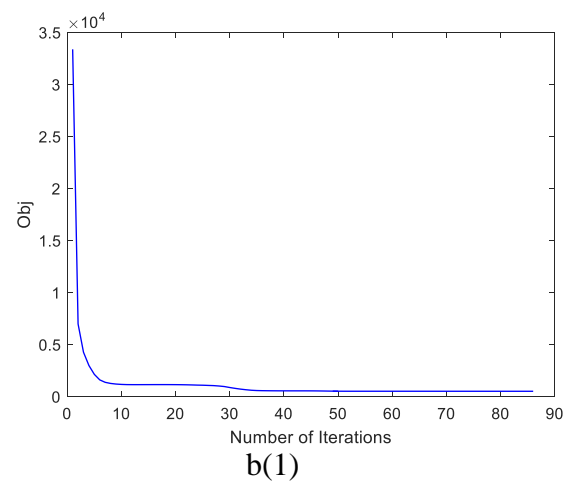
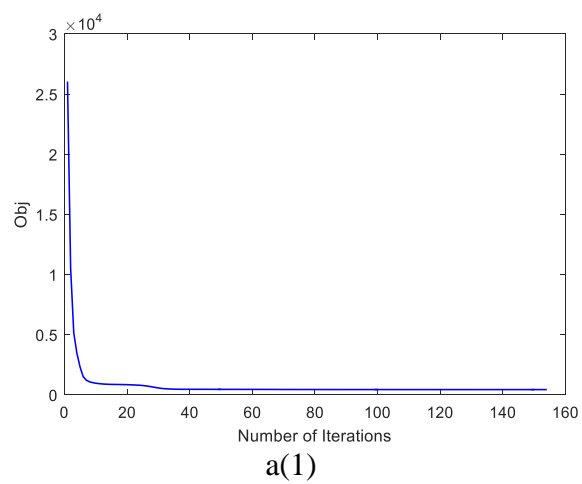
b(3)



a(4)

b(4)

Fig. 11 Optimized results in macro and micro scales for Michelle-type structure  
(left: deterministic design; right: uncertain design)





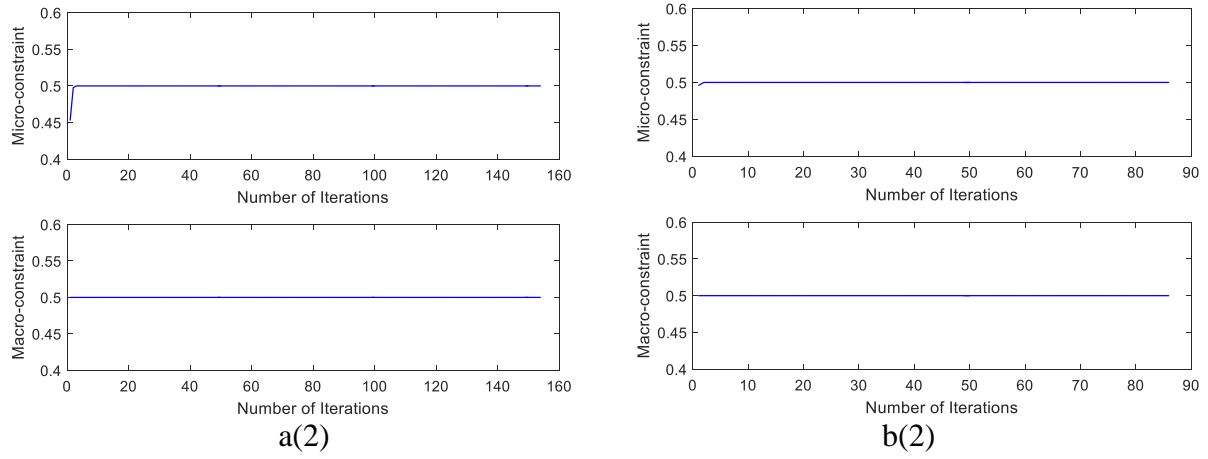


Fig. 12 Convergent history for Michelle-type structure  
(left: deterministic design; right: uncertain design)

## 5. Conclusion

This paper has proposed a new robust topology optimization method for the integrated material-structural designs subject to random-interval uncertainties, which includes a hybrid univariate dimension reduction (HUDR) method to estimate the interval mean and interval variance of the objective function. The numerical examples have demonstrated that the uncertainties have obvious influence on the optimized designs both at macro and micro scales, and the robust designs obtained by using the proposed method are better than the deterministic designs. The numerical results have also shown that the proposed method has good computational efficiency and accuracy. The proposed method is actually a general approach that can be applied to any topology optimization problems involving hybrid uncertainties. It is noted that the proposed uncertain propagation method may not be adequate for problems with high non-linearity and strong correlation amongst uncertain parameters. In the future, we will focus on how to extend the uncertain analysis method to deal with more advanced design problems with high non-linearity and strong correlation.

## Acknowledgments

This research is partially supported by the National Natural-Science-Foundation of China (51575204, 51705166), the Australian Research Council (ARC) - Discovery Projects (160102491), and the National Science Foundation for Distinguished Young Scholars of China (51725502).

## References

- [1] Bendsøe MP, Kikuchi N. Generating optimal topologies in structural design using a homogenization method. *Comput Methods Appl Mech Eng* 1998; 71(2): 197-224.
- [2] Bendsøe MP, Sigmund O. Material interpolation schemes in topology optimization. *Arch Appl Mech* 1999; 69(9-10): 635-654.
- [3] Sigmund O. A 99 line topology optimization code written in Matlab. *Struct Multidiscip Optim* 2001; 21(2): 120-127.
- [4] Xie YM, Steven GP. A simple evolutionary procedure for structural optimization. *Comput Struct* 1993; 49(5): 885-896.

- [5] Huang X, Xie YM. Bi-directional evolutionary topology optimization of continuum structures with one or multiple materials. *Comput Mech* 2009; 43(3): 393-401.
- [6] Sethian JA, Wiegmann A. Structural boundary design via level set and immersed interface methods. *J Comput Phys* 2000; 163(2): 489-528.
- [7] Wang MY, Wang X, Guo D. A level set method for structural topology optimization. *Comput Methods Appl Mech Eng* 2003; 192(1): 227-246.
- [8] Allaire G, Jouve F, Toader AM. Structural optimization using sensitivity analysis and a level-set method. *J Comput Phys* 2004; 194(1): 363-393.
- [9] Amstutz S, Andrä H. A new algorithm for topology optimization using a level-set method. *J Comput Phys* 2006; 216(2): 573-588.
- [10] Deaton JD, Grandhi RV. A survey of structural and multidisciplinary continuum topology optimization: post 2000. *Struct Multidiscip Optim* 2014; 49(1): 1-38.
- [11] Sigmund O, Maute K. Topology optimization approaches. *Struct Multidiscip Optim* 2013; 48(6): 1031-1055.
- [12] Zhang WH, Xia L, Zhu JH, Zhang Q. Some recent advances in the integrated layout design of multicomponent systems. *J Mech Des* 2011; 133(10): 104503.
- [13] Gibson LJ, Ashby MF. *Cellular solids: structure and properties*. Cambridge university press; 1999.
- [14] Sigmund O. A new class of extremal composites. *J Mech Phys Solids*, 2000; 48(2): 397-428.
- [15] Andreassen E, Lazarov BS, Sigmund O. Design of manufacturable 3D extremal elastic microstructure. *Mech Mater* 2014; 69(1): 1-10.
- [16] Wang YQ, Luo Z, Zhang N, Kang Z. Topological shape optimization of microstructural metamaterials using a level set method. *Comput Mater Sci* 2014; 87: 178-186.
- [17] Zhang WH, Sun SP. Scale-related topology optimization of cellular materials and structures. *Int J Numer Meth Eng* 2006; 68(9): 993-1011.
- [18] Podshivalov L, Fischer A, Bar-Yoseph P Z. On the road to personalized medicine: multiscale computational modeling of bone tissue. *Arch Comput Method E* 2014; 21(4): 399-479.
- [19] Li H, Luo Z, Gao L, et al. Topology optimization for concurrent design of structures with multi-patch microstructures by level sets. *Comput Methods Appl Mech Eng* 2018; 331: 536-561.
- [20] Yan J, Yang SX, Duan ZY, Yang CQ. Minimum compliance optimization of a thermoelastic lattice structure with size-coupled effects. *J Therm Stress* 2015; 38(3): 338-357.
- [21] Yan J, Guo X, Cheng GD. Multi-scale concurrent material and structural design under mechanical and thermal loads. *Comput Mech* 2016; 57(3): 437-446.
- [22] Rodrigues H, Guedes JM, Bendsoe MP. Hierarchical optimization of material and structure. *Struct Multidiscip Optim* 2002; 24(1): 1-10.
- [23] Liu L, Yan, J, Cheng GD. Optimum structure with homogeneous optimum truss-like material. *Comput Struct* 2008; 86(13): 1417-1425.
- [24] Fujii D, Chen BC, Kikuchi N. Composite material design of two-dimensional structures using the homogenization design method. *Int J Numer Meth Eng* 2001; 50(9): 2031-2051.
- [25] Deng JD, Yan J, Cheng GD. Multi-objective concurrent topology optimization of thermoelastic structures composed of homogeneous porous material. *Struct Multidiscip Optim*, 2013; 47(4): 583-597.
- [26] Vicente WM, Zuo ZH, Pavanello R, Calixto TKL, Picelli R, Xie YM. Concurrent topology optimization for minimizing frequency responses of two-level hierarchical structures. *Comput Methods Appl Mech Eng* 2016; 301: 116-136.
- [27] Li H, Luo Z, Zhang N, Gao L, Brown T. Integrated design of cellular composites using a level-set topology optimization method, *Comput Methods Appl Mech Eng* 2016; 309: 453-475.
- [28] Fragiadakis M, Papadrakakis M. Modeling, analysis and reliability of seismically excited structures: computational issues. *Int J Comp Meth*, 2008; 5(4): 483-511.
- [29] Ben-Haim Y, Elishakoff I. *Convex models of uncertainty in applied mechanics*. Amsterdam: Elsevier; 2013.
- [30] Moore RE. *Interval analysis*. Englewood Cliffs: Prentice-Hall; 1996.
- [31] Ferson S, Kreinovich V, Ginzburg L, Myers DS, Sentz K. *Constructing probability boxes and Dempster-Shafer structures*. Sandia National Laboratories, Albuquerque; 2002.
- [32] Jiang C, Zheng J, Han X. Probability-interval hybrid uncertainty analysis for structures with both aleatory and epistemic uncertainties: a review. *Struct Multidiscip Optim* 2017; 1-18.
- [33] Du XP. Interval reliability analysis. Proceedings of ASME 2007 International Design Technical Conferences and Computers and Information in Engineering Conference, Las Vegas, Nevada, 2007.
- [34] Xia BZ, Yu DJ, Liu J. Hybrid uncertain analysis of acoustic field with interval random parameters. *Comput Methods Appl Mech Eng* 2013; 256: 56-69.

- [35] Wang C, Qiu ZP. Hybrid uncertain analysis for steady-state heat conduction with random and interval parameters. *Int J Heat Mass Transf* 2015; 80: 319-328.
- [36] Wu D, Gao W. Hybrid uncertain static analysis with random and interval fields. *Comput Methods Appl Mech Eng* 2017; 315: 222-246.
- [37] Huang ZL, Jiang C, Zhou YS, Zheng J, Long XY. Reliability-based design optimization for problems with interval distribution parameters. *Struct Multidiscip Optim* 2016; 1-16.
- [38] Jiang C, Zheng J, Ni BY, Han X. A probabilistic and interval hybrid reliability analysis method for structures with correlated uncertain parameters. *Int J Comp Meth* 2015; 12(4): 1540006.
- [39] Jiang C, Li WX, Han X, Liu LX, Le PH. Structural reliability analysis based on random distributions with interval parameters. *Comput Struct* 2011; 89(23): 2292-2302.
- [40] Penmetsa RC, Grandhi RV. Efficient estimation of structural reliability for problems with uncertain intervals. *Comput struct* 2002; 80(12): 1103-1112.
- [41] Wu JL, Luo Z, Zhang N, Zhang YQ. A new uncertain analysis method and its application in vehicle dynamics. *Mech Syst Signal Process* 2015; 50: 659-675.
- [42] Rahman S, Xu H. A univariate dimension-reduction method for multi-dimensional integration in stochastic mechanics. *Probabilist Eng Mech*, 2004; 19(4): 393-408.
- [43] Chen SH, Ma L, Meng GW, Guo R. An efficient method for evaluating the natural frequencies of structures with uncertain-but-bounded parameters. *Comput Struct*, 2009; 87(9): 582-590.
- [44] Maute K. Topology Optimization under uncertainty. In *Topology Optimization in Structural and Continuum Mechanics*. Springer Vienna; 2014; 457-471.
- [45] Guo X, Cheng GD. Recent development in structural design and optimization. *Acta Mechanica Sinica* 2010; 26(6): 807-823.
- [46] Kharmanda G, Olhoff N, Mohamed A, Mohamed A, Lemaire M. Reliability-based topology optimization. *Struct Multidiscip Optim* 2004; 26(5): 295-307.
- [47] Kim C, Wang S, Rae K, Moon H, Choi KK. Reliability-based topology optimization with uncertainties. *J Mech Sci Technol* 2006; 20(4): 494-504.
- [48] Kanakasabai P, Dhingra A K. An efficient approach for reliability-based topology optimization. *Eng Optimiz* 2016; 48(1): 1-15.
- [49] Jalalpour M, Tootkaboni M. An efficient approach to reliability-based topology optimization for continua under material uncertainty. *Struct Multidiscip Optim* 2016; 53(4): 759-772.
- [50] Du JB, Sun CC. Reliability-based vibro-acoustic microstructural topology optimization. *Struct Multidiscip Optim* 2017; 55(4): 1195-1215.
- [51] Csébfalvi A. Robust Topology Optimization: A New Algorithm for Volume-constrained Expected Compliance Minimization with Probabilistic Loading Directions using Exact Analytical Objective and Gradient. *Periodica Polytechnica Civil Engineering* 2016; 61(1), 154-163.
- [52] Zhao JP, Wang CJ. Robust structural topology optimization under random field loading uncertainty. *Struct Multidiscip Optim* 2014; 50(3): 517-522.
- [53] Chen SK, Chen W, Lee S. Level set based robust shape and topology optimization under random field uncertainties. *Struct Multidiscip Optim* 2010; 41(4): 507-524.
- [54] da Silva GA, Cardoso EL. Stress-based topology optimization of continuum structures under uncertainties. *Comput Methods Appl Mech Eng* 2017; 313: 647-672.
- [55] Luo YJ, Kang Z, Luo Z, Li A. Continuum topology optimization with non-probabilistic reliability constraints based on multi-ellipsoid convex model. *Struct Multidiscip Optim* 2009; 39(3): 297-310.
- [56] Xu B, Zhao L, Xie YM, Jiang J. Topology optimization of continuum structures with uncertain-but-bounded parameters for maximum non-probabilistic reliability of frequency requirement. *J Vib Control* 2015; 1077546315618279.
- [57] Zhang XP, Kang Z, Zhang WB. Robust topology optimization for dynamic compliance minimization under uncertain harmonic excitations with inhomogeneous eigenvalue analysis. *Struct Multidiscip Optim* 2016; 54(6): 1469-1484.
- [58] Guo X, Zhao XF, Zhang WS, Yan J, Sun GM. Multi-scale robust design and optimization considering load uncertainties. *Comput Methods Appl Mech Eng*, 2015; 283: 994-1009.
- [59] Wu JL, Luo Z, Li H, Zhang N. Level-set topology optimization for mechanical metamaterials under hybrid uncertainties. *Comput Methods Appl Mech Eng* 2017; 319, 414-441.
- [60] Chen N, Yu DJ, Xia BZ, Ma ZD. Topology optimization of structures with interval random parameters. *Comput Methods Appl Mech Eng* 2016; 307: 300-315.

- [61] Sigmund O. Materials with prescribed constitutive parameters: An inverse homogenization problem. *Int J Solids Struct*, 1994; 31(17): 2313-2329.
- [62] Andreassen E, Andreassen CS. How to determine composite material properties using numerical homogenization. *Comp Mater Sci* 2014; 83: 488-495.
- [63] Hassani B, Hinton E. A review of homogenization and topology optimization I-homogenization theory for media with periodic structure. *Comput Struct* 1998; 69(6): 707-717.
- [64] Haug EJ, Choi KK, Komkov V. *Design sensitivity analysis of structural systems*. Orlando: Academic Press; 1986.
- [65] Madsen HO, Krenk S, Lind NC. *Methods of structural safety*. Courier Corporation, 2006.
- [66] Rozvany GIN, Bendsøe MP, Kirsch U. Layout Optimization of Structures. *Appl Mech Rev* 1995; 48(2): 41-119.
- [67] Sigmund O. On the design of compliant mechanisms using topology optimization. *J Struct Mech* 1997; 25(4): 493-524.

Table 1 Results of multi-scale topology optimization for cantilever beam

	Mean	Standard deviation	Robust objective function	Effective elasticity tensor	Convergence iterations	FEA calls
Deterministic design (HUDR)	619.7488	95.8351	715.5839	$\begin{bmatrix} 0.3497 & 0.0758 & 0.0245 \\ 0.0758 & 0.0982 & 0.0212 \\ 0.0245 & 0.0212 & 0.0778 \end{bmatrix}$	134	35
Deterministic design (MCS)	621.0812	96.0135	717.0947			$10^7$
Uncertain design (HUDR)	569.2122	87.7946	657.0068	$\begin{bmatrix} 0.3538 & 0.0793 & 0.0182 \\ 0.0793 & 0.1443 & 0.0179 \\ 0.0182 & 0.0179 & 0.0774 \end{bmatrix}$	136	35
Uncertain design (MCS)	570.4529	87.9659	658.4190			$10^7$

Table 2 Results of multi-scale topology optimization for MBB beam

	Mean	Standard deviation	Robust objective function	Effective elasticity tensor	Convergence iterations	FEA calls
Deterministic design (HUDR)	$1.1797 \times 10^3$	166.7591	$1.3465 \times 10^3$	$\begin{bmatrix} 0.3813 & 0.0577 & -0.0001 \\ 0.0577 & 0.0778 & -0.0001 \\ -0.0001 & -0.0001 & 0.0632 \end{bmatrix}$	96	35
Deterministic design (MCS)	$1.1796 \times 10^3$	166.3731	$1.3460 \times 10^3$			$10^7$
Uncertain design (HUDR)	$1.0864 \times 10^3$	152.6211	$1.2390 \times 10^3$	$\begin{bmatrix} 0.3886 & 0.0619 & 0.0013 \\ 0.0619 & 0.1106 & 0.0010 \\ 0.0013 & 0.0010 & 0.0618 \end{bmatrix}$	99	35
Uncertain design (MCS)	$1.0862 \times 10^3$	152.3253	$1.2385 \times 10^3$			$10^7$

Table 3 Results of multi-scale topology optimization for Michelle-type structure

	Mean	Standard deviation	Robust objective function	Effective elasticity tensor	Convergence iterations	FEA calls
Deterministic design (HUDR)	507.9243	58.4620	556.3863	$\begin{bmatrix} 0.2126 & 0.0717 & 0.0003 \\ 0.0717 & 0.2687 & 0.0004 \\ 0.0003 & 0.0004 & 0.0643 \end{bmatrix}$	154	70
Deterministic design (MCS)	507.8067	58.3730	566.1797			$10^7$
Uncertain design (HUDR)	463.6389	53.3526	516.9915	$\begin{bmatrix} 0.2458 & 0.0800 & 0.0029 \\ 0.0800 & 0.2757 & 0.0035 \\ 0.0029 & 0.0035 & 0.0706 \end{bmatrix}$	86	70
Uncertain design (MCS)	463.6422	53.2107	516.8529			$10^7$